ANALYSIS OF V TRANSMISSION LINES RESPONSE TO EXTERNAL ELECTROMAGNETIC FIELDS

A. Cheldavi and P. Nayeri

College of Electrical Engineering
Iran University of Science and Technology
Narmak, Tehran, 16844, Iran

Abstract—In the present paper the response of V transmission line to electromagnetic illumination has been obtained. Also in order to determine the VTL frequency operation band for both TE and TM modes a Gaussian pulse source has been applied to the structure. The VTL structure has received considerable attention in high frequency and microwave IC packaging. The purpose of this study is to determine high frequency design considerations in order to reduce the effects of electromagnetic interference (EMI) on the VTL structure and maintain the desired performance. It was observed that the effect of incident EM waves on the V lines performance is considerably lower than conventional microstrips, however the V lines are more sensitive to sources at close proximity. In addition, although the V lines show lower dispersion at higher frequencies, their frequency operation band is limited by a resonance like behavior which is directly related to the V groove dimensions. The full wave analysis is carried out using the Yee-cell based 2 Dimensional Finite Difference Time Domain method (2D-FDTD), while enforcing a very stable and efficient mesh truncation technique.

1. INTRODUCTION

Recently, the V-shaped transmission line (VTL) has been the subject of growing interest as it has presented a solution to technical and technological problems encountered in the design of microstrip lines. It has the ability to operate without the need for via-holes and also provides further design advantages, such as reduced radiation loss and sensitivity and the availability of a wide range of impedances. The geometry of the line is essentially a microstrip in which the ground

plane is bent within the dielectric in a V shape to form the sides of an isosceles triangle. A typical V line structure is depicted in Fig. 1.
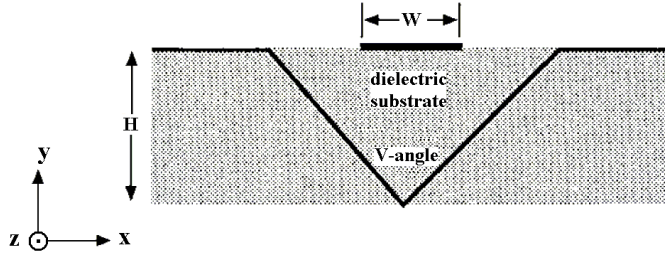
Figure 1. Cross section of the V line structure.

The VTL structure has far been analyzed using different methods [1–5], while assuming quasi-TEM field behavior. However under these quasi static assumptions, important propagation features (full wave effects) are not accounted for. Most importantly these interconnects are used in high frequency and microwave IC packaging. With the clock speed reaching far into the GHz region, the exact knowledge of the effect of incident electromagnetic waves on the transmission lines performance is of critical importance, due to the need to predict and control EMI between neighboring components in high density packaging. In this work, we extend the analysis of the V line structure to the GHz regime, where it cannot be predicted by quasi static methods. This analysis is expedited by using the 2D-FDTD method.

2. FORMULATION

The Yee algorithm solves for both electric and magnetic fields in time and space using the coupled Maxwell's curl equations, rather than solving for the electric field alone (or the magnetic field alone) with a wave equation. Using both E and H information, the solution is more robust than using either alone. The FDTD method has been applied to the analysis of microstrip line structures and there are many excellent papers on the use of FDTD in TL structures (see [7, 8]). Therefore the details of the FDTD method are henceforth bypassed. For the application of our work we focus on our modeling aspects, the mesh truncation scheme, and various sources representing incident electromagnetic fields.

The nonrectangular sections in the FDTD model can be modeled using two different techniques, the stair-case technique and the polygonal approximation (used to model curved metal boundaries)

[12]. The later has a potential for instability in resonant structures requiring very large number of time steps, therefore the modeling of the ground plane present in the V line structure is done using the stair-case technique. The next step is to consider a computational domain large enough to enclose the structure, and a suitable boundary condition on the outer perimeter of the domain to simulate its extension to infinity. The implementation of a good mesh truncation technique is highly important in all open-region FDTD simulations, therefore we use the Perfectly Matched Uniaxial Medium (UPML). The uniaxial material performs as well as Berenger's PML while avoiding the nonphysical field splitting. This anisotropic medium is uniaxial, and is composed of both electric and magnetic permittivity tensors. Implementing the UPML as a single step-discontinuity of σ_e and σ_m in the FDTD lattice can lead to significant spurious wave reflection at the UPML surface. To reduce the reflection error of the Absorbing Boundary Condition (ABC) we use a number of UPML layers with a polynomial grading. Polynomial grading is simply

$$k_x(x) = 1 + \left(\frac{x}{d}\right)^m \cdot (k_{x,\max} - 1) \qquad (1)$$

Typically, $3 < m < 4$ has been found to be nearly optimal for many FDTD simulations. This increases the value of the k_x of the UPML from 0 at the surface of the UPML to $k_{x,\max}$ at the PEC outer boundary (d is the total depth of the UPML layer and η is the impedance of each layer). For the polynomial grading the parameters can be readily determined for a given desired reflection error $R(0)$.

$$k_{x,\max} = -\frac{(m+1)\ln[R(0)]}{2\eta d} \qquad (2)$$

The ABC's enforced on the boundaries lead to highly reliable results as demonstrated in the section of numerical results. The FDTD computational domain is shown in Fig. 2.

The final step is the excitation of the TL with electromagnetic fields. A point wise hard source located within a 2D-FDTD grid excites a radially propagating cylindrical wave centered on the source point. However, comparison of the FDTD calculations with the exact analytical solutions have shown that the point wise source has a range of effective action radius of 0.2 grid cell in 2D-FDTD models [11], therefore the size of the grid has to be considerably small in order to create a proper point source. A continuous sinusoidal wave with the desired frequency can also be modeled in the 2 dimensional grid as a line source. For this excitation scheme the important consideration is achieving the sinusoidal steady state, which is done by using a sufficient number of time steps relative to the excitation frequency.
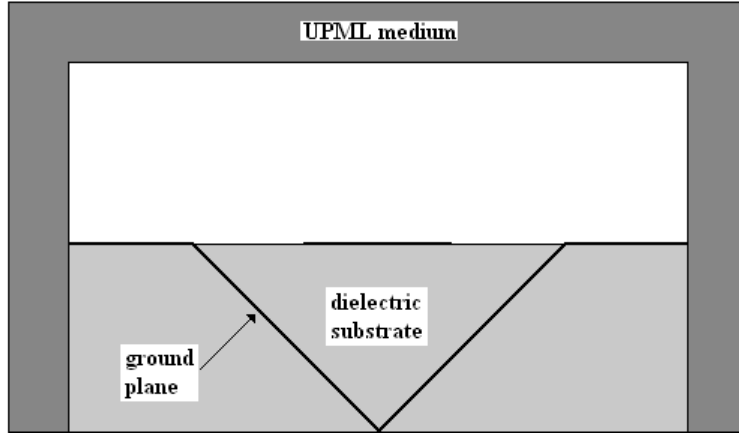
Figure 2. FDTD computational domain.

3. NUMERICAL RESULTS

The dimension of the FDTD square cells were chosen $\Delta = 0.02\,\text{mm}$ to provide a minimum grid sampling density of 20 samples at the highest frequency considered. To avoid reflection from the artificial boundaries we have used a 10 layer UPML medium with polynomial grading. The Courant factor is set to 0.75 which corresponds to a time step of $\Delta t = 0.035\,\text{ps}$.

As an example of a V line structure, we consider a line with the following dimensions.

1) Width of the signal line, $W = 0.4\,\text{mm}$
2) Height of the substrate, $H = 0.6\,\text{mm}$
3) Substrate Dielectric constant, $\varepsilon_r = 2.54$
4) Thickness of the signal strip is assumed to be negligible.

Note that, in this text VTL-α corresponds to a V line structure with a V-angle of α degrees (Fig. 1).

3.1. Electromagnetic Illumination

Example 1.

To observe the V lines response to an incident sinusoidal wave and to compare it with the ordinary microstrip, we expose the V line and a conventional microstrip line with the same dimensions $(w/h) = 0.66$ to a sinusoidal wave with excitation frequency of $3\,\text{GHz}$, TM_z polarization

and electrical field strength of $E_0 = 1\,\mathrm{V/m}$. To achieve steady state at this frequency the simulation is continued until $1\,\mathrm{ns}$.

These simulations (Fig. 3) show that the electric field inside the dielectric of the microstrip reaches the steady state considerably sooner than the V line, clearly indicating that the field inside the dielectric of the V line is less sensitive to external waves than the microstrip. The main reason for such a behavior is the limited dielectric-air interface in the V line structure which prevents the penetration of the EM fields into the substrate.
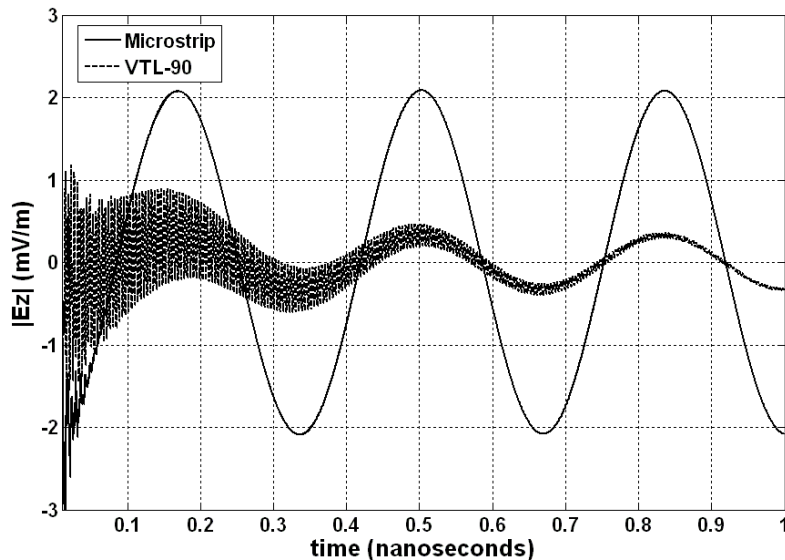
Figure 3. Electric field inside the dielectric, TM_z mode.

The magnitude of the induced current distribution along the strip width due to incident electromagnetic fields is an important parameter in determining the electromagnetic capabilities of the transmission line. Both microstrip and VTL structures are exposed to a sinusoidal wave with TM_z polarization, electrical field strength of $E_0 = 1\,\mathrm{V/m}$ and excitation frequency of $3\,\mathrm{GHz}$. The induced current distribution on the strips is calculated for various V angles and w/h ratios ($\varepsilon_r = 2.54$).

These results show that the V line structure is less affected by the external waves than the microstrip and by reducing the V angle the magnitude of the induced current will decrease. For the TE_z polarization, the same sinusoidal wave source with unity amplitude and normal incidence is considered and the magnitude of the electric field ($|E_x|$) inside the dielectric ($\varepsilon_r = 2.54$) is compared with the microstrip
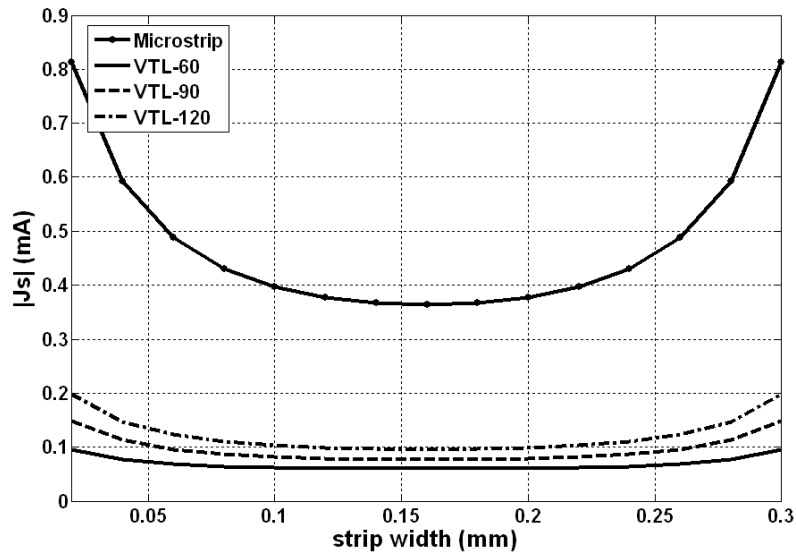
Figure 4a. Induced current on the strips, $w/h = 0.46$.
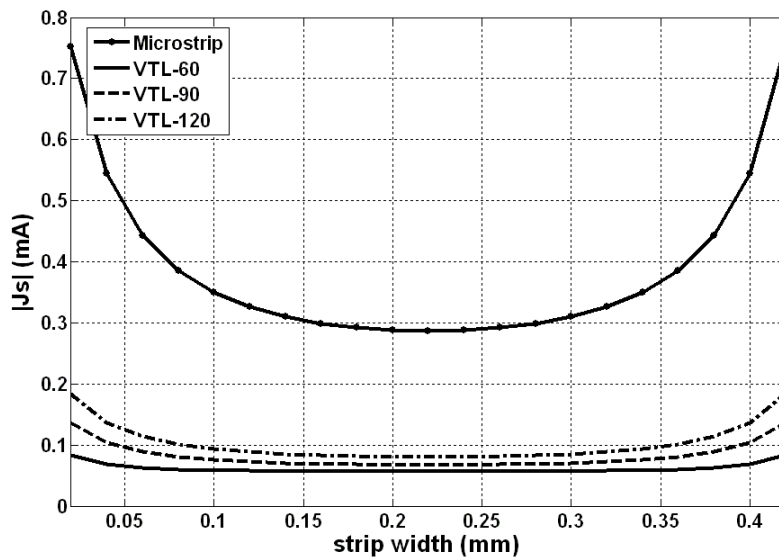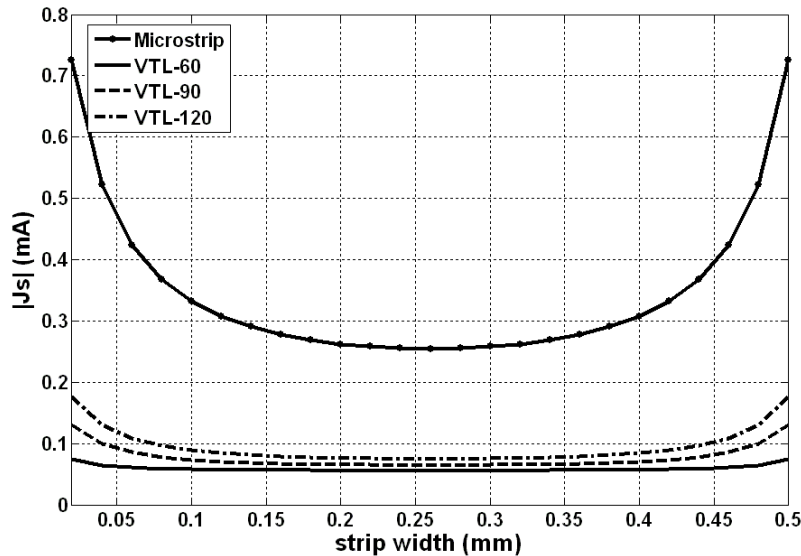

Figure 4b. Induced current on the strips, $w/h = 0.66$.

Figure 4c. Induced current on the strips, $w/h = 0.8$.

at 1 ns (Fig. 5).

It can be seen that the magnitude of the electric field inside the VTL is considerably less than the microstrip. The tangential electric field is essentially zero on the strip and the ground plane, therefore a maximum will generally be expected around the mid-height of the substrate. This maximum value is closer to the strip for all microstrip configurations [13]. For the V lines the field is directly related to the V angle, therefore similar to the TM_z case, a V line with a smaller V-angle will be less sensitive to electromagnetic exposure.

Example 2.

An important excitation scheme in electromagnetics is the presence of a line source in the near field. To observe both the V line and microstrip responses to such a source we place a line source above the strip. This source considered here excites a radially propagating sinusoidal cylindrical wave with electrical field strength of $E_0 = 1\,\text{V/m}$ and excitation frequency of 3 GHz.

Without the loss of generality this line source is positioned directly above the center of the strip ($d = 0.6\,\text{mm}$). The induced current distribution on the strip is calculated for the TM_z mode at 1 ns for various V angles (Fig. 7).

It is observed that the VTL structure is very sensitive to sources in
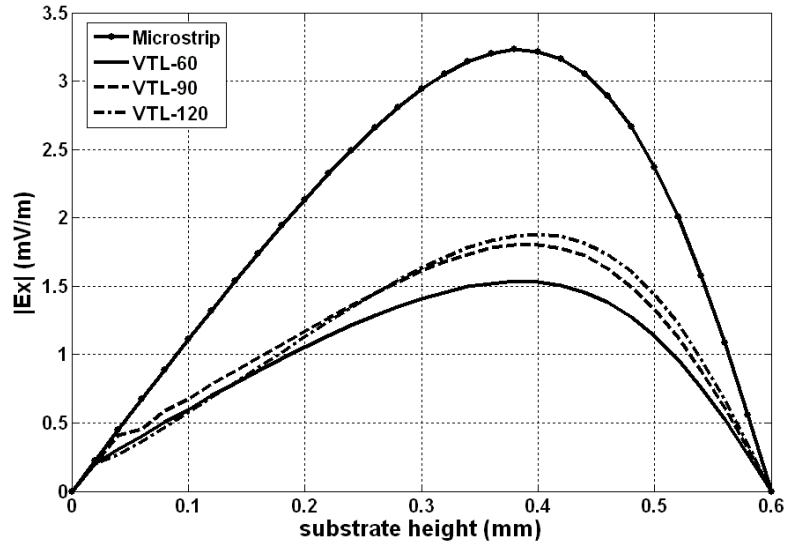
**Figure 5.** Electric field inside the dielectric region of the VTL and microstrip $(w/h = 0.66)$.
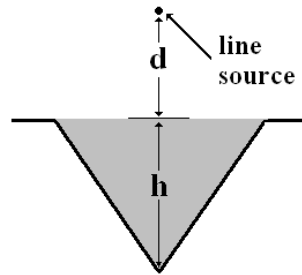
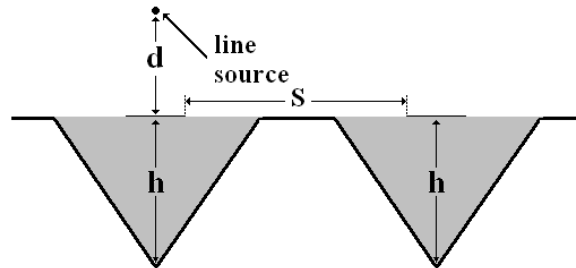**Figure 6.** Excitation by a line source in the 2DFDTD model.

the near field region. This behavior is due to the fact that the presence of a source in the near field greatly excites the fields in the substrate especially the fields corresponding to the transmission lines dominant modes, therefore the induced current will be greatly increased. We should also point out that in the case of near field excitation increasing the V angle would reduce the induced current on the strips, therefore from the EMI point of view it might be better to use V lines with larger V angles if external sources are at close proximity relative to the wavelength.

A primary interest in the V line structure is its coupling
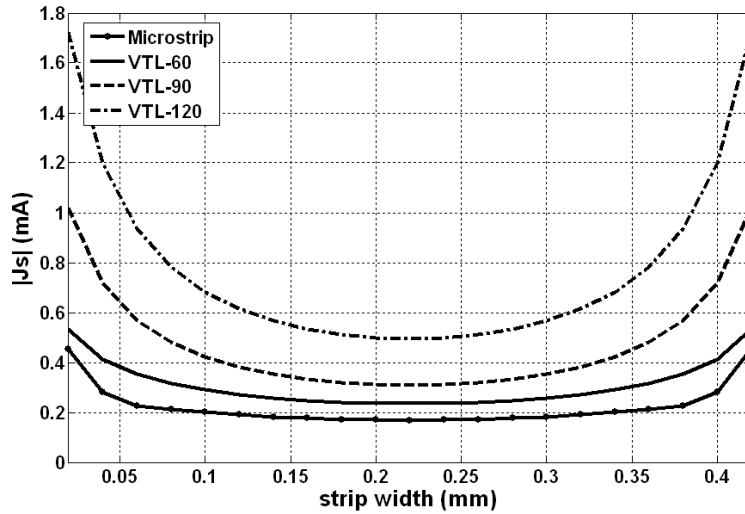
Figure 7. Induced current on the strips, $w/h = 0.66$, Excitation by line source.


Figure 8. Excitation by a line source (multi-conductor).

characteristics when two or more lines are placed in a multi-conductor configuration as shown in Fig. 8. This coupled line structure is excited with the same line source which is positioned directly above the center of the first strip ($d = 0.6$ mm).

The induced current distribution on the adjacent strip is calculated at 1 ns for both coupled V line and microstrip configurations with $s = 1$ mm (Fig. 9).

It is observed that the induced current on the adjacent strip is considerably lower for the V line structure, which indicates a lower coupling between the lines. Generally for coupled line microstrip structures, the induced current on the adjacent strip approaches a
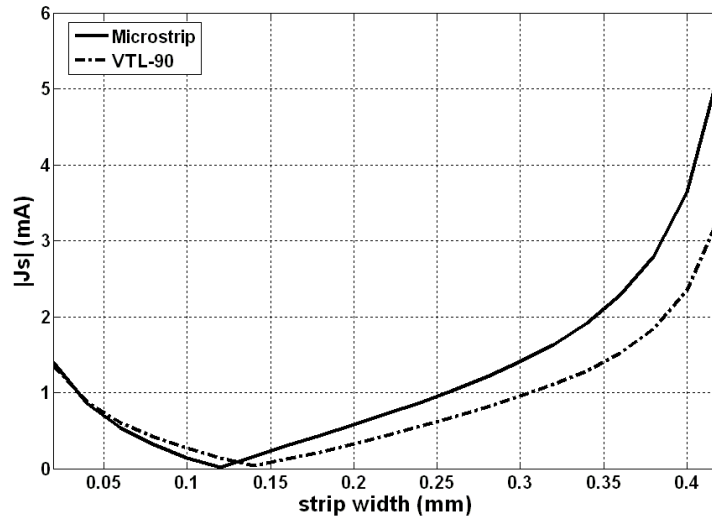
Figure 9. Induced current on the second strip for VTL and microstrip ($w/h = 0.66$, $s/w = 2.5$).

minimum value at a distance closer to the source, not at the center of the strip. However for V lines, the ground planes alter the position of this minimum and it occurs at an even closer distance to the source (in compare with microstrips). Therefore in the case of multi-conductor structures the V lines perform considerably better than the conventional microstrips. This feature makes the V line very attractive for high density packaging in which EMC considerations are extremely important.

3.2. Frequency Operation Band

To observe the V lines response to a high frequency pulse we consider a line source (Fig. 6) with a Gaussian pulse. The Gaussian pulse is described by the following equation

$$f(t) = e^{-\frac{t^2}{\sigma^2}} \tag{3}$$

where σ is a rough measure of the pulse width. This point wise hard source is positioned directly above the strip ($d = 0.6$ mm) and the pulse duration is 1 ps. The resulting electric field distribution is shown in Fig. 10 for the TM_z mode at 12 ps.

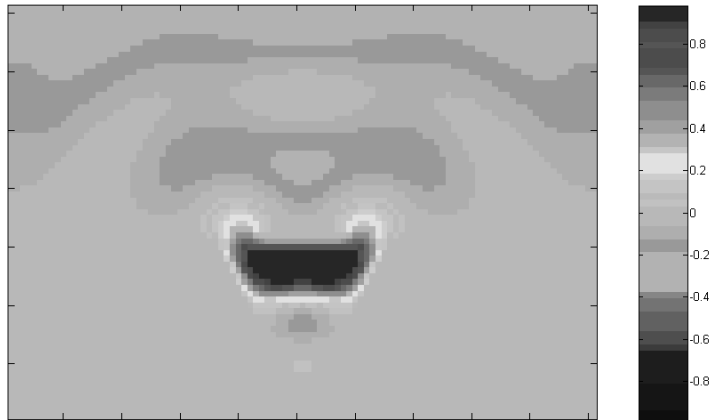Similar results can be obtained for the TE_z mode. The magnetic field distribution is shown in Fig. 11.

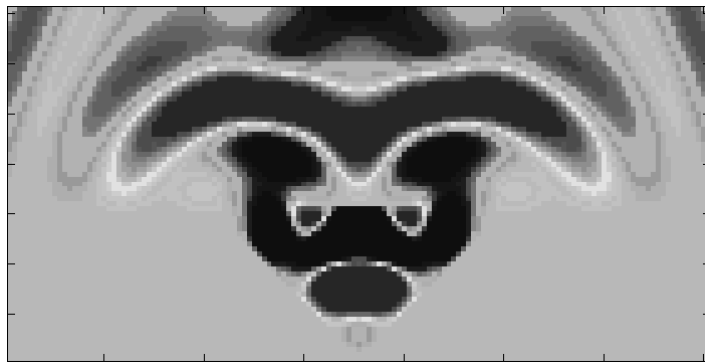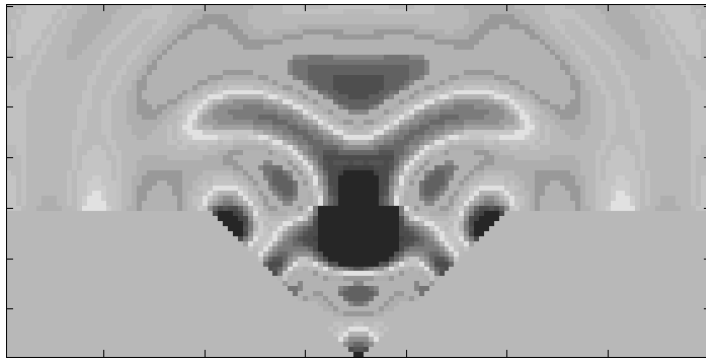**Figure 10a.** E_z at 12 ps, $V = 60$ degrees, $w/h = 0.66$.

Figure 10b. E_z at 12 ps, $V = 90$ degrees, $w/h = 0.66$.
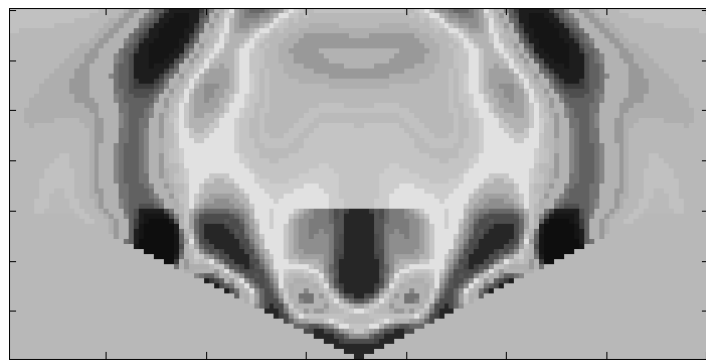

Figure 10c. E_z at 12 ps, $V = 120$ degrees, $w/h = 0.66$.

Figure 11a. H_z at 12 ps, $V = 60$ degrees, $w/h = 0.66$.

Figure 11b. H_z at 12 ps, $V = 90$ degrees, $w/h = 0.66$.

Figure 11c. H_z at 12 ps, $V = 120$ degrees, $w/h = 0.66$.

It is observed that the field distribution in the VTL structure is greatly influenced by the V-angle. Namely for the 60° V-groove the magnitude of the electromagnetic fields inside the substrate is considerably lower, which indicates lower EMI. Also for 90° and 120° V-grooves, these field distributions are quite different. i.e., the 120° structure shows almost continuous electromagnetic fields inside the dielectric and above the interface, where as for the 90° structure these continuous fields are not observed, mainly because of the smaller dielectric-air interface. Therefore we would generally expect the V angle to have characteristic effect on the V lines performance.

A powerful strength of the FDTD method is that it can give the desired field functions over a very wide band of frequencies with a single computer simulation. To obtain the desired spectrum the wave form of the incident wave should excite as many frequencies as possible, which is done using a standard Gaussian excitation. For our simulations we use a Gaussian point wise source with a pulse rise time of 1 ps, sufficient enough for predicting frequency responses up to 400 GHz. In order to minimize high frequency errors this pulse is shifted in time such that its peak occurs at $t = 3$ ps. This point wise source is positioned directly above the center of the strip (Fig. 6) and would be removed from the equations after it has completely decayed. The pulse wave form is shown in Fig. 12.

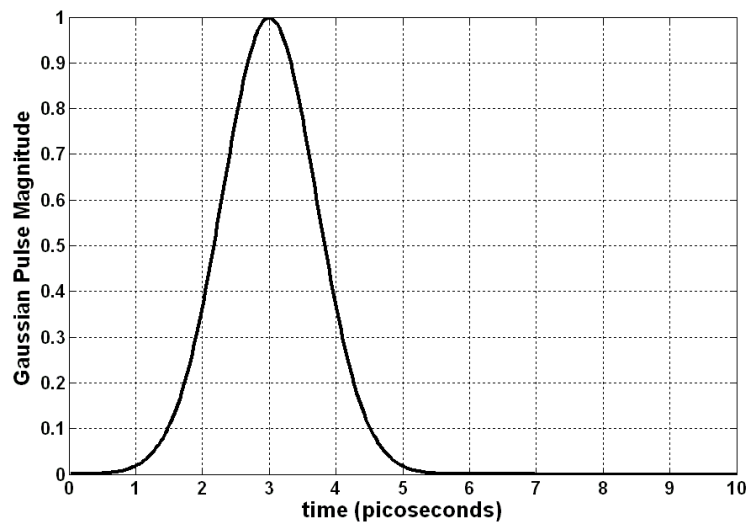We notice that both the V line structure and the microstrip

Figure 12. Gaussian pulse waveform in the time domain.

exhibit a resonance like behavior at high frequencies. This implies that
relatively high energy is being transferred to the line at this frequency.
Generally the resonant like behavior of the microstrip does not need to
be considered, because it occurs at very high frequencies in which the
microstrip cannot perform well because of high frequency dispersion
effects. On the other hand for the V line these dispersion effects
are considerably lower and they don't limit the lines performance [6],
therefore we need to study these resonance behaviors.

It was observed that the resonance point magnitude decreased
greatly with increasing the V angle, therefore the normalized power
spectrums are shown in Figs. 13, 14 for structures with $w/h = 0.66$
and a dielectric constant of 2.54. We should also mention that this
resonance behavior was observed at all points inside the dielectric
substrate but with different magnitudes.
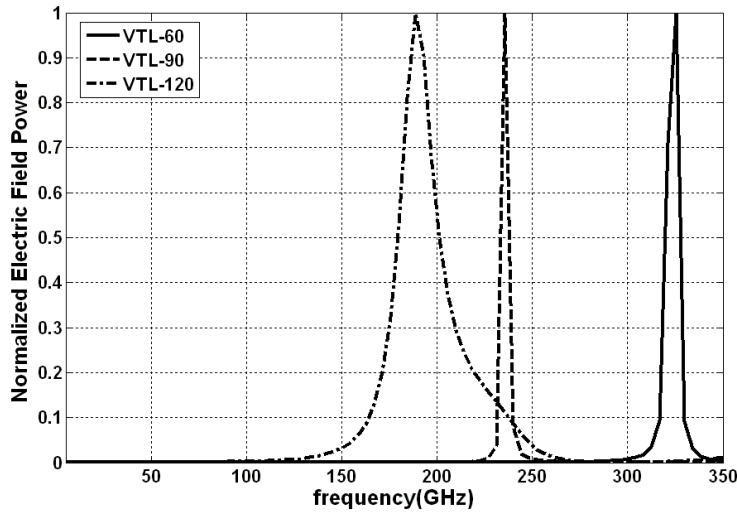
Figure 13. Normalized power spectrum of the electric field inside the
dielectric (TM_z mode).

The power spectrum of the TM_z mode (Fig. 13), shows the
resonance like behavior occurs at frequencies around 320, 240 and
180 GHz for V lines with 60, 90 and 120 degrees V angles respectively.
Considerably different from this case, the TE_z power spectrum
(Fig. 14) shows resonant behavior occurring at frequencies around
70 GHz for all lines.

Generally the resonance point in these structures must be directly
related to the V groove. In fact a series of simulations showed that for
the TM_z mode the resonance point is directly related to the V angle
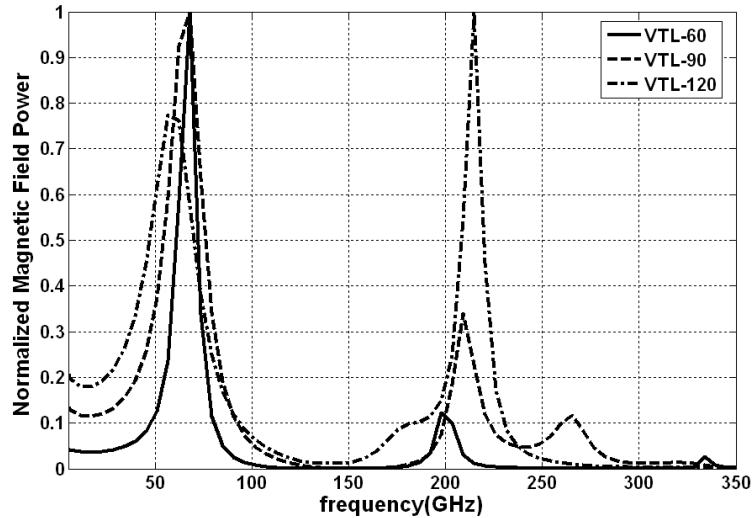
Figure 14. Normalized power spectrum of the magnetic field inside the dielectric (TE_z mode).

and that it occurs at frequencies corresponding to approximately twice the V groove opening (wavelength in the dielectric medium should be considered here). This was further verified by increasing the dielectric constant, which would decrease the resonance point (Fig. 15).

For the TE_z mode our simulations indicate that this resonance behavior is directly related to the height of the substrate. A series of simulations showed that the first resonance occurs at wavelengths corresponding to approximately 4 times the substrate height (wavelength in the dielectric medium should be considered here). The effect of dielectric constant on the resonance point is presented in Fig. 16.

The TE_z power spectrum (Fig. 14) also shows that a second resonance occurs around 200 GHz. The secondary TE_z resonance is due to the reflection which occurs under the strip. This trend was verified by removing the strip. In this case the second resonance will be completely removed (Fig. 17).

We should also note that the TE_z mode is much more sensitive to external electromagnetic fields as it shows considerably high power delivered to the system at even very low frequencies. This minimum power will be reduced by decreasing the V angle (Fig. 14), therefore from the EMI point of view it is recommended to use V lines with smaller V angles.
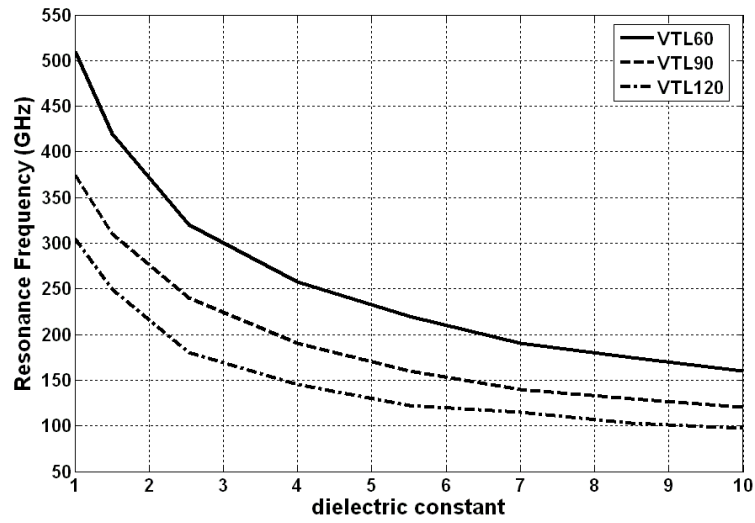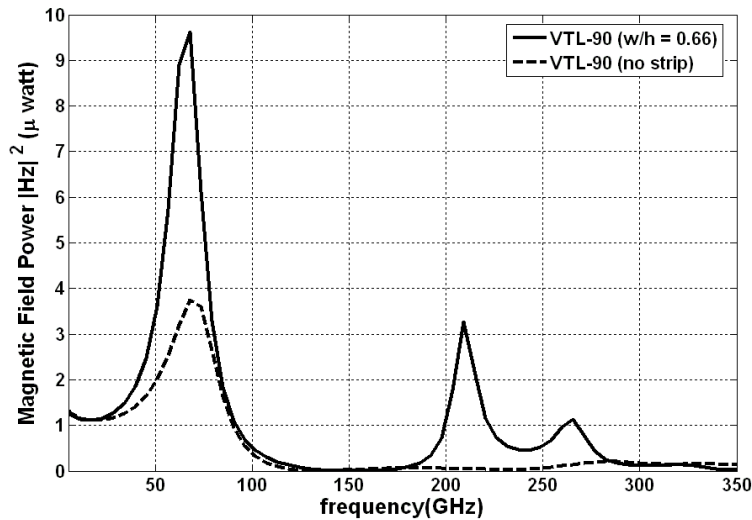
Figure 15. Effect of dielectric constant on the Resonance point (TM_z mode).
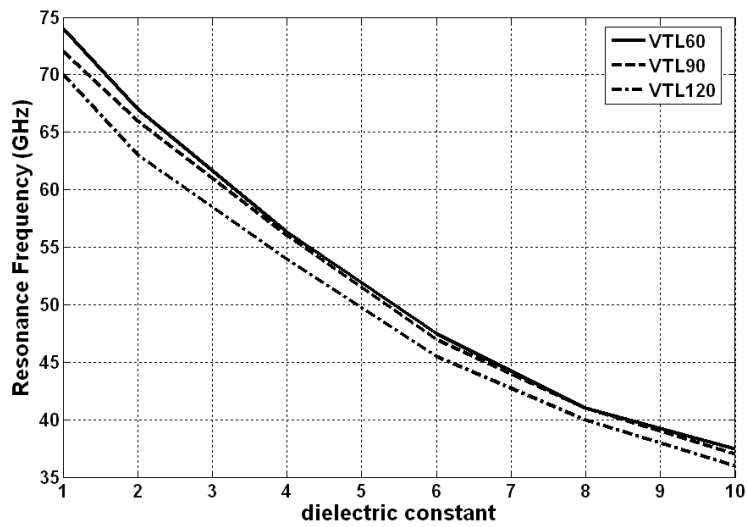
Figure 16. Effect of dielectric constant on the Resonance point (TE_z mode).

Figure 17. Effect of removing the strip on the Resonance point (TE_z mode).

For both modes our simulations showed that the w/h ratio has very little effect on the resonance point. Generally the trace plays the role of cavity loads thus altering the resonance point [6], but in these structures the first resonance point is directly related to the V groove dimensions. It is possible however that the trace will alter the higher resonance modes.

Due to this resonance like behavior, the operation of V lines at high frequencies has to be considered properly. Clearly the application of the V lines does not call for the V grooves to be efficient radiators, therefore the resonant frequencies will limit the operation band of the line. The resonant behavior for TM_z modes occurs at very high frequencies and might not be important, because this frequency range is of little interest. On the other hand the TE_z mode resonant behavior occurs at much lower frequencies which should be considered as the highest limit of the V line frequency operation band.

4. CONCLUSION

In this work, the 2D Yee-cell based FDTD method was used to study the effects of electromagnetic illumination and also high frequency design considerations of the V line. Both TE_z and TM_z polarization modes are analyzed and the results are compared with conventional

microstrip. It is observed that the V line performs much better than the microstirp under far field electromagnetic exposure. On the other hand the VTL structure is very sensitive to sources in the near field region, however for the case of multi-conductor structures, lower coupling of the V lines greatly reduces EMI on adjacent lines. The frequency operation band of VTL structures was also obtained in this study and is limited by their resonance behavior in the TE_z mode. This full wave analysis shows that the VTL structure is considerably superior to microstrips from EMI point of view and this behavior is maintained till very high frequencies. This feature makes the V line very attractive for high density and microwave IC packaging.

REFERENCES

1. Schutt-Aine, J. E., "Static analysis of V transmission lines," *IEEE Trans. Microwave Theory Tech.*, Vol. MTT-40, No. 4, 659–664, Apr. 1992.

2. Asheh, C. B., D. Bhattacharya, and R. Garg, "Characterization of V-groove coupled microshield line," *IEEE Micro. Wireless Comp. Letters*, Vol. 15, No. 2, 110–112, Feb. 2005.

3. Yuan, N. C., C. L. Ruan, and W. G. Lin, "Analytical analyses of V, elliptic, and circular-shaped microshield transmission lines," *IEEE Trans. Microwave Theory Tech.*, Vol. MTT-42, No. 5, 855–859, May 1994.

4. Keshmiri, F., G. Dadashzadeh, A. Cheldavi, and P. Nayeri, "A Novel method for analysis of V-transmission lines," *Antem/Ursi*, July 16–19, 2006.

5. Cheldavi, A. and P. Nayeri, "Circualr symmetric multiconductor V-shaped transmission line: A new type fo microwave interconnects," *J. of Electromagnetic Waves and Appl.*, Vol. 20, No. 4, 461–474, 2006.

6. Ramahi, O. M., A. Z. Elsherbeni, and C. E. Smith, "Dynamic analysis of V transmission lines," *IEEE Trans. Comp. Packaging and Man. Tech.*, Vol. 21, No. 3, 250–257, Aug. 1998.

7. Xiao, S., R. Vahldieck, and H. Jin, "Full-wave analysis of guided wave structures using a novel 2-D FDTD," *IEEE Microwave Guide Wave Lett.*, Vol. 2, 165–167, May 1992.

8. Sheen, D. M., S. M. Ali, M. D. Abouzahra, and J. A. Kong, "Application of the three-dimensional finite-difference time-domain method to the analysis of planar microstrip circuits," *IEEE Trans. Micorwave Theory Tech.*, Vol. 38, 849–857, July 1990.

9. Taflove, A. and S. Hagness, *Computational Electrodynamics: The Finite Difference Time Domain Method*, 2nd ed., Artech House, 2000.

10. Sadiku, M. N. O., *Numerical Techniques in Electromagnetics*, 2nd ed., 186–190, CRC Press LLC., FL, 2001.

11. Waldschmidt, T., "Range of effective action radius of a hard source field component in a 2D-FDTD grid," *IEEE Microwave & Guided Wave Lett.*, 217–219, 2000.

12. Mezzanotte, P., L. Roselli, and R. Sorrentino, "A simple way to model curved metal boundaries in FDTD algorithm avoiding staircase approximation," *IEEE Microwave Guide Wave Lett.*, Vol. 5, 267–269, Aug. 1995.

13. Balanis, C. A., *Advanced Engineering Electromagnetics*, 444–457, John Willey & Sons, 1989.